



ACCEPTED ON ANNALS OF GEOPHYSICS, 61, 2018; Doi:  
10.4401/ag-7782

## Far-field boundary conditions in channeled lava flow with viscous dissipation

Marilena Filippucci<sup>1\*</sup>, Andrea Tallarico<sup>1</sup>, Michele Dragoni<sup>2</sup>

<sup>1</sup>Dipartimento di Scienze della Terra e Geoambientali, Università di Bari, Via Orabona 4, 70125 Bari, Italy.

<sup>2</sup>Dipartimento di Fisica e Astronomia, Università di Bologna - Alma Mater Studiorum, Viale Carlo Berti Pichat 8, 40127 Bologna, Italy.

# 1 **Far-field boundary conditions in channeled lava flow with viscous** 2 **dissipation**

3 M. Filippucci<sup>1\*</sup>, A. Tallarico<sup>1</sup>, M. Dragoni<sup>2</sup>

4 <sup>1</sup>*Dipartimento di Scienze della Terra e Geoambientali, Università di Bari, Via Orabona 4, 70125*  
5 *Bari, Italy.*

6 <sup>2</sup>*Dipartimento di Fisica e Astronomia, Università di Bologna - Alma Mater Studiorum, Viale Carlo*  
7 *Berti Pichat 8, 40127 Bologna, Italy.*

8  
9 Key-words: Rheology, Magmas, Thermodynamics, Lava flow, Viscous dissipation, Solid boundary

## 10 **ABSTRACT**

11 Cooling and dynamics of lava flowing in a rectangular channel driven by the gravity force is  
12 numerically modeled. The purpose is to evaluate the thermal process as a function of time involving  
13 the liquid lava in contact with the solid boundary that flanks lava. Lava rheology is dependent on  
14 temperature and strain rate according to a power law function. The model couples dynamics and  
15 thermodynamics inside the lava channel and describes the thermal evolution of the solid boundary  
16 enclosing the channel. Numerical tests indicate that the solution of the thermo-dynamical problem  
17 is independent of the mesh. The boundary condition at the ground and at the levees is treated  
18 assuming a solid boundary around the lava flow across which lava can exchange heat by  
19 conduction. A far field thermal boundary condition allows to overcome the assumption of constant  
20 temperature or constant heat flow as boundary conditions, providing more realistic results. The  
21 effect of viscous heating is evaluated and discussed.  
22

## 23 **Introduction**

24 Laboratory studies have extensively demonstrated that lava rheology under certain conditions  
25 including vesicularity (Stein and Spera, 1992; Badgassarov and Pinkerton, 2004), crystalline  
26 concentration (Pinkerton and Stevenson, 1992; Smith, 2000; Sonder et al., 2006; Champallier et al.,  
27 2008) and in a certain temperature range (Shaw et al., 1968) assumes non-Newtonian pseudoplastic  
28 properties.

29 When the problem of lava flowing under the effect of gravity is resolved, the power law rheology  
30 introduces a non-linearity in the diffusion term of the momentum equation and consequently an  
31 analytical solution of the differential equations governing the motion does not exist. Furthermore, if  
32 the viscosity function also includes temperature dependence, the thermal equation is coupled to the  
33 dynamic equation. Hence the need to solve numerically the thermo-dynamic equations describing  
34 the flows of a fluid as complex as lava.

35 In the thermal modeling of lava flows, the greatest difficulties are due to the different thermal  
36 exchanges both external (surface thermal radiation, forced convection, conduction at the base) and  
37 internal (axial advection, viscous dissipation, latent heat, internal conduction) to be taken into  
38 account. Despite the great progress made in numerical modeling, it is necessary to assume some  
39 simplifying hypotheses.

40 The need for simplifying assumptions in numerical models of lava flows is described in review  
41 articles (Costa and Macedonio, 2005b; Cordonnier et al., 2015; Dietterich et al., 2017). The authors  
42 examine the most relevant works on the numerical modeling of lava flows and what emerges is that,  
43 due to the high complexity of transport equations, the numerical solution of the complete three-  
44 dimensional problem for real lava flows is often intractable. This has led to concentrate the main  
45 efforts on the development of software able to quickly describe the evolution of a lava flow, based  
46 on simplified theoretical models, for the purpose of volcanic hazard assessment.

47 Parallel to the development of general numerical models closely linked to volcanic hazard, it is  
 48 necessary to study the details of what happens when, during an effusive process, a fluid like lava  
 49 flows in a channel.

50 Filippucci et al. (2017) discussed the problem of viscous dissipation in channeled lava flows and  
 51 found that the effect of viscous heating is irrelevant for the most of the channel domain apart from  
 52 the boundaries where some temperature differences were noticed. These temperature differences  
 53 brought the authors to hypothesize that the fluid motion can lose the laminarity at the boundary  
 54 (since locally the Reynolds number exceeds the laminar/turbulent threshold). The same effect was  
 55 found by Costa and Macedonio (2005) who found that the fluid can develop secondary flows at the  
 56 boundaries as an effect of viscous heating.

57 In dealing with problems involving the heat equation, in this case coupled to the momentum  
 58 equation by the rheological function, the boundary condition for a channeled flow is classically  
 59 chosen between constant temperature and constant heat flow (Patankar, 1980; Ferziger and Peric,  
 60 2002).

61 From the observation that the effect of viscous heating is observed only at the boundaries, in this  
 62 paper we considered a third possibility, that is a conductive solid boundary with which the fluid can  
 63 exchange heat. In particular, in this paper we focus on the thermal process involving the liquid lava  
 64 in contact with the solid edges of the channel, assuming that the fluid can cool down by losing heat  
 65 by conduction in the hosting rocks and by radiation in the atmosphere and can heat up by the effect  
 66 of heat advection and viscous dissipation. Some authors (Costa et al., 2007; Filippucci, 2018) used  
 67 far-field boundary conditions to model the thermal interaction between the hot fluid flow and the  
 68 host rock with numerical methods. Similarly, in this work, the solid boundary condition is treated  
 69 realistically considering that the rock that hosts the lava flow can exchange heat by conduction.

## 70 **Mathematical problem**

71 The constitutive equation for a power law fluid is

$$\sigma_{ij} = 2k\dot{\epsilon}^{n-1}\dot{\epsilon}_{ij} \quad (1)$$

72 where  $\sigma_{ij}$  is the stress tensor,  $\dot{\epsilon}_{ij}$  is the strain rate tensor,  $k$  is the fluid consistency,  $n$  is the power  
 73 law exponent which is a measure of nonlinearity, and

$$\dot{\epsilon} = 2\sqrt{|I_2|} \quad (2)$$

74 where  $I_2$  is the second invariant of the strain rate tensor. The apparent viscosity  $\eta_a$  of the fluid is

$$\eta_a = k\dot{\epsilon}^{n-1} \quad (3)$$

75 If  $n$  is lower than 1, the fluid is pseudoplastic and it thins with an increase in stress. If  $n$  is equal to  
 76 1, the fluid is Newtonian. If  $n$  is greater than 1, the fluid is dilatant and it thickens with an increase  
 77 in stress (White, 2005).

78 We assume a viscous fluid flowing in the  $x$  direction in a rectangular conduit inclined at an angle  $\alpha$ ,  
 79 perpendicularly to the section of the conduit in the  $yz$  plane. The channel is surrounded by edges of  
 80 solid material of thickness  $a_s$  with which it can exchange heat by conduction.

81 The channel width is  $2a$ , thickness  $h$  and length  $L$ . The sketch of the model with the coordinate  
 82 system is shown in Figure 1 and the values of the parameters are listed in Table 1.

83 The flow is laminar and subjected to the gravity force. Pressure changes are negligible with respect  
 84 to body forces. The velocity is approximately axial and varies with the lateral coordinates  $v_x(y,z)$ ,  $v_y$   
 85  $=0$ ,  $v_z=0$ . The fluid is isotropic and incompressible with constant density  $\rho$ , thermal conductivity  $K$ ,  
 86 specific heat capacity  $c_p$ .

87 The equation of motion in the transient state for a gravity driven flow down an inclined rectangular  
 88 channel is (Filippucci et al., 2013a):

$$\rho \frac{\partial v_x}{\partial t} = \rho g \sin \alpha + \frac{\partial}{\partial y} \left( \eta_a \frac{\partial v_x}{\partial y} \right) + \frac{\partial}{\partial z} \left( \eta_a \frac{\partial v_x}{\partial z} \right) \quad (4)$$

89 where  $v_x$  is the  $x$  component of velocity,  $g$  is the gravity acceleration and  $\alpha$  is the slope angle. The  
 90 apparent viscosity is (Filippucci et al., 2005):

$$\eta_a = k \left[ \left( \frac{\partial v_x}{\partial y} \right)^2 + \left( \frac{\partial v_x}{\partial z} \right)^2 \right]^{\frac{n-1}{2}} \quad (5)$$

91  
92  
93  
94  
95  
96  
97  
98  
99  
100  
101  
102  
103  
104  
105  
106  
107  
108  
109  
110  
111  
112  
113  
114  
115  
  
116  
  
117  
  
118  
119  
120  
121  
122  
  
123  
124  
125  
126  
127  
128  
129  
130  
131  
132  
133  
134  
135  
136  
137

where  $v_x$  is the  $x$  component of velocity and both the fluid consistency  $k$  and the power law exponent  $n$  depend on temperature. The temperature dependence of  $k$  and  $n$  is given by Hobiger et al. (2011):

$$k(T) = K_0 e^{p_1 + \frac{p_2}{T}} \quad (6)$$

$$n(T) = 1 + p_3 + p_4 T \quad (7)$$

where  $k_0$ ,  $p_1$ ,  $p_2$ ,  $p_3$  and  $p_4$  are constant parameters listed in Table 1.

The numerical problem of the dynamics of lava flows was already detailed, by studying the sensitivity of the solution to the variation of the power law exponent  $n$  and to the fluid consistency  $k$  (Filippucci et al, 2010; 2011; 2013b), by using a temperature-dependent power-law rheology and analyzing the thermal effects due to heat advection (Filippucci et al. 2013a) and to viscous dissipation (Filippucci et al., 2017). The problem of the solid boundaries has been considered by Filippucci (2018).

We assume that the fluid flow is transient, laminar and subjected to the gravity force. Downflow pressure changes are negligible with respect to the body force. Since the channel cross section is rectangular and the Reynolds number is low almost everywhere in the domain (Filippucci et al., 2017), the assumption of laminar flow implies that the velocity is approximately axial, but it may depend on all the coordinates:  $v_x = v_x(x, y, z)$ .

Differently to the approach of Filippucci (2018), we include the effect of viscous dissipation as an internal heat source. We neglect the effect of the latent heat of crystallization/fusion.

The boundary conditions are the no-slip at the walls and the zero-stress at the top of the flow. Since the solution is computed in a half domain of width  $a/2$ , thickness  $h$  and length  $L$ , we consider as boundary condition the symmetry of the problem with respect to the  $xz$  plane. So, the boundary conditions are the following:

$$v_x(x = 0) = v_x(T_e) \quad (8)$$

$$v_x(\pm a_l, z) = 0; \quad v_x(y, -h_l) = 0 \quad (9)$$

$$\frac{\partial v_x}{\partial y}(0, z) = 0; \quad \frac{\partial v_x}{\partial z}(y, 0) = 0 \quad (10)$$

The initial condition for velocity is the steady state numerical solution at the initial effusion temperature  $v_x(x, y, z, t = 0) = v_x(T_e)$ .

The time dependent heat equation inside the channel takes into account the effect of thermal exchange by heat advection, conduction and viscous dissipation:

$$\rho c_p \frac{\partial T}{\partial t} + \rho c_p v_x \frac{\partial T}{\partial x} = K \left( \frac{\partial^2 T}{\partial y^2} + \frac{\partial^2 T}{\partial z^2} \right) + \eta_a \left[ \left( \frac{\partial v_x}{\partial y} \right)^2 + \left( \frac{\partial v_x}{\partial z} \right)^2 \right] \quad (11)$$

We can neglect the effect of thermal conduction in the flow direction as it is of secondary importance with respect to thermal advection in the flow direction (Filippucci et al., 2013a).

The time dependent heat equation outside the channel, in the solid boundary, is purely conductive:

$$\rho c_p \frac{\partial T}{\partial t} = K \left( \frac{\partial^2 T}{\partial y^2} + \frac{\partial^2 T}{\partial z^2} \right) \quad (12)$$

The thermal boundary conditions are the assumptions of a radiative heat flux  $q_r$  at the upper flow surface, a constant temperature  $T_w$  at the outer solid walls (such a far field condition is imposed at a distance equal to three times the half-width of the channel), a constant effusion temperature  $T_e$  at the vent and the symmetry of the problem with respect to the  $xz$  plane:

$$T(x = 0) = T_e \quad (13)$$

$$T(x = 0, y = \pm a, z = -h) = T_w \quad (14)$$

$$\frac{\partial T}{\partial y}(y = 0) = 0 \quad (15)$$

$$\frac{\partial T}{\partial z}(-a_l < y < a_l, z = 0) = -\frac{q_r}{K} \quad (16)$$

where  $q_r = \sigma \varepsilon T_u^4$  and  $\sigma$  is the Stefan-Boltzmann constant,  $\varepsilon$  is the surface emissivity of lava and  $T_u$  is the temperature of the upper surface at  $z = 0$  (the atmospheric temperature is assumed negligible with respect to  $T_u$ ).

At time  $t = 0$ , the liquid lava has a uniform temperature  $T_e$ , the velocity is the stationary solution of the dynamic equation with  $T = T_e$  and the outer solid boundary has uniform temperature  $T_w$ . The choice of the initial condition was made in order to compare this solution with that of Filippucci et al. (2017). Moreover, the assumption of the extrusion temperature of the fluid as starting condition in numerical studies is widely used and accepted in finite element/volume modeling (Costa and Macedonio, 2003; Patrick, 2004; Bernabeu et al, 2016; among others).

At time  $t > 0$ , the radiative heat flux  $q_r$ , the far field constant temperature  $T_w$  and the constant effusive temperature  $T_e$  are imposed. Since  $x = L$  is the outflow boundary and both temperature and velocity need to be computed there, no boundary condition at  $x = L$  is necessary.

The dynamic and the thermal equation are coupled by the temperature dependence of viscosity in the dynamic equation and by the viscous dissipation term in the heat equation. The algorithm is written by the authors in Fortran language. The space discretization is obtained by the control volume integration method (Patankar, 1980) using a static mesh approach and power law interpolation functions between the nearest grid points. The radiative condition at the boundary  $z = 0$  depends on the fourth power of temperature and needs to be linearized in order to be treated as a source term of the heat equation. For the discretization of the transient term, the integration over the time interval  $t$  is made by using a fully implicit scheme. The iterative solver of the discretized equation is the Gauss-Seidel one (Filippucci et al., 2013a, for details of the flow chart procedure).

The solution is tested to verify the independence of the mesh and the test is shown in Figure 2. The computational problem was solved by considering three grids of different sizes ( $52 \times 52$ ,  $102 \times 102$ ,  $202 \times 202$ ) to discretize the  $(y, z)$  section, transversal to the fluid direction. The space discretization along the  $x$  direction was fixed to 101 control volumes. The time solution is stopped at  $t = 10^6$  s since for long times the temperature approaches the steady-state solution. The channel geometry for the numerical test is described by the parameters in Table 1. The temperature profile along the  $z$  coordinate at the outflow boundary slightly varies with varying the mesh size, indicating that the problem is independent of the control volume size.

As expected, the finest mesh ( $201 \times 201$ ) needs a very large computational cost to achieve the convergence, which means a long time for calculation. In the following, for the problem with geometrical parameters listed in Table 1, the mesh  $y \times z \times x = 102 \times 102 \times 101$  was used as the best compromise between accuracy and computation time. In particular, in this case, the computational time is approximately 2 days of computation for the problem with the viscous dissipation term, and approximately 1 day for the solution without the viscous dissipation term.

## Results and discussion

The problem is illustrated in Figure 1 with the physical and geometrical parameters given in Table 1. We have evaluated the temperature distribution in an inclined lava channel flanked by solid levees, with which the flowing lava interacts thermally: while lava cools down, the levees are heated in turn. Results are obtained considering that the lava cools by thermal radiation at the free surface and by thermal conduction at the solid boundaries. Moreover, the lava can be heated by the effect of viscous dissipation. The solid surrounding rocks, in turn, heat up by thermal conduction.

187 The problem is transient, and the first  $10^6$  s (approximately 1 day) are modeled, assuming that at  $t =$   
188 0 the whole channel has a temperature  $T$  equal to the effusion temperature  $T_e$  and the levees have  
189 uniform wall temperature  $T_w$ .

190 The choice of the distance of the constant temperature boundary condition is arbitrary. Costa et al.  
191 (2007) used a far-field temperature at an arbitrary distance of 10 times the radius of the magma  
192 conduit. Our choice is dictated as a compromise between far-field and computational time costs.  
193 This choice can be considered adequate since, after  $t = 10^6$  s of cooling, the boundary is still not  
194 heated, as it can be seen in Figure 3a.

195 In a previous paper, Filippucci (2018) has numerically solved the same problem, but neglecting the  
196 viscous dissipation term in the heat equation. In Figure 3b, we plotted the difference with the  
197 solution of Filippucci (2018) in terms of temperature  $T(y, z)$  map in the vertical cross section at the  
198 outflow boundary ( $x = L$ ) at  $t = 10^6$  s. It can be observed that the viscous dissipation term has an  
199 effect in the parts of the lava channel in contact with the boundaries and the ground. If we consider  
200 the whole lava channel, the effect of viscous heating can be considered of secondary importance  
201 with respect to the advective term. If we consider the behavior of the fluid in contact with the solid  
202 edges, the heat addition due to viscous dissipation can bring the fluid flow to change the motion  
203 from laminar to locally turbulent (Filippucci et al., 2017) and to develop secondary flows (Costa  
204 and Macedonio, 2003, 2005a)

205 In Figure 4, we plotted the temperature variation with time at 8 monitoring points (P1, ..., P8)  
206 selected inside the lava channel and corresponding to the black points in Figure 4A. If we observe  
207 the temperature evolution with time at some points of the channel section in the flow outlet area  
208 (Figure 4), we realize that there are fluid regions that are almost at constant temperatures equal to  
209 those of  $T_e$  and areas with temperature that oscillates without differences between dissipative and  
210 non-dissipative case with the exception of point P5 in contact with the ground at the center of the  
211 channel. At points P1, P6 and P8, temperature remains constant and equal to that of effusion  $T(t) =$   
212  $T_e$  during the prescribed time. At these points, the temperature difference between the dissipative  
213 and non-dissipative case are in the order of tenths of a centigrade degree. At point P2, temperature  
214 decreases monotonically during the first  $10^3$  s approximately and then remains constant for the  
215 following time. The effect of viscous dissipation is to dampen the cooling process and to allow the  
216 fluid to be at a constant higher temperature in less time. At points P3, P4 and P7, the temperature  
217 has an oscillating behavior in time: at first it decreases and then returns to increase without  
218 significant differences between the dissipative and non-dissipative case and with a greater  
219 oscillation amplitude at point P4 than in the other points. At point P5, the temperature behavior with  
220 time is similar to the one just described, but in this case the difference between dissipative and non-  
221 dissipative case is sharper.

222 The main difference with the work of Filippucci et al. (2017) and then between boundary conditions  
223 with constant temperature gradient and far field boundary conditions, where temperature gradient is  
224 free to vary as a function of the thermal conduction rate, is just shown in Figure 4 (points P3, P4, P5  
225 and P7).

226 In fact, at the same points, in the case of boundary condition with constant heat flux, temperature  
227 increases monotonically in the presence of viscous dissipation, while it decreases monotonically in  
228 the absence of dissipation (Fig. 7 in Filippucci et al., 2017). Considering far field boundary  
229 conditions, the temperature initially decreases and after a certain time internal it starts to increase  
230 and this oscillation is independent from the viscous dissipation term in the heat equation.

231 This oscillation can be interpreted considering that, as the lava flow is emplaced, the difference in  
232 temperature between the host rocks and the hosted lava is so high that it causes a very intense  
233 conductive heat flow. This flow cools the lava in contact with rocks, as shown by the descending  
234 part of the curves in Figure 4 (points P3, P4, P5 and P7). Over time, the host rocks heat up as a  
235 result of heat conduction and the heat flow begins to decrease and so does the cooling rate of the  
236 lava in contact with rocks, leading to the minimum of the curves in Figure 4 (points P3, P4, P5 and  
237 P7). Continuing with time, the conductive heat flow becomes no longer the dominant mechanism,  
238 since advective heating begins to prevail due to the isothermal core at the center of the channel, that  
239 flows with temperature equal to that of effusion. This change in heat transfer mechanism leads the  
240 hosted lava in contact with the host rocks to heat up, as shown by the ascending part of the curves in

241 Figure 4 (points P3, P4, P5 and P7). The effect of viscous dissipation during the described thermal  
242 process is that of reducing the oscillation amplitude Figure 4 (points P5).  
243

## 244 **Conclusions**

245 The purpose of this work is to investigate how the choice of boundary conditions may affect the  
246 results of a model of a channeled lava flow, in particular by evaluating the importance of the  
247 viscous dissipation term. To do this, we developed a flow model with far-field constant temperature  
248 boundary conditions, allowing the liquid lava to exchange heat with the host solid rock. The results  
249 were compared with those obtained in a previous work (Filippucci et al., 2018) in which the cooling  
250 at the levees and at the ground was modeled by imposing a constant conductive heat flow. With the  
251 model presented in this paper, we go beyond the classical boundary conditions at the channel walls,  
252 which assume constant temperature or constant heat flow, usually adopted in works dealing with  
253 lava flow simulation, as reviewed by Costa and Macedonio (2005b). Far field boundary conditions  
254 are more realistic since it is not necessary to impose a constant temperature nor an arbitrary  
255 constant temperature gradient at the channel levees and at the ground.

256 We solved numerically the dynamic and heat equations of a lava flowing by gravity inside a  
257 channel with rectangular cross section, flanked by a thick solid levee, by using the finite volume  
258 method (Patankar, 1980).

259 The dynamic equation is solved only in the liquid domain, while the heat equation is solved both in  
260 the liquid and in the solid domain. The viscous dissipation term is considered in the heat equation.  
261 The solution was tested in order to verify that the convergence of the numerical problem is  
262 independent of the mesh size. The results indicate that the solid edge interacts with the liquid lava,  
263 both at the levees and the ground, causing an initial cooling due to heat conduction and a  
264 subsequent heating due to heat advection. This thermal process is not affected by viscous  
265 dissipation, which only acts by decreasing the temperature variation interval between the cooling  
266 and the heating process. On the contrary, when the boundary condition at the levees and at the  
267 ground is a constant temperature gradient (Filippucci et al., 2017) or a constant temperature (Costa  
268 et al., 2007), the effect of viscous dissipation at the boundaries appears to be of great importance,  
269 causing an increase of the Reynolds number from laminar to turbulent values (Filippucci et al.,  
270 2017) and triggering secondary flows (Costa et al., 2007).

271 Filippucci (2018), using the same far field boundary conditions but neglecting viscous heating,  
272 found that the channel levees can melt, since they can heat over the solidus temperature. In this  
273 work, including viscous dissipation, we observe the same thermal behavior of the edge (**Figure 3a**),  
274 but the effect of thermal erosion cannot be evaluated quantitatively. In order to analyze melting of  
275 the solid edges and changes in the channel morphology, we should adopt a moving boundary, so as  
276 to account that portions of the host rocks may pass from solid to liquid behavior and, vice versa,  
277 portions of lava in the channel may pass from liquid to solid behavior. As reviewed by Costa and  
278 Macedonio (2005b), works dealing with lava flows impose that the channel boundaries are taken at  
279 constant temperature or at constant temperature gradient. Differently, far field thermal boundary  
280 condition allows to overcome this simplification and makes the physical treatment of the problem  
281 more realistic.  
282

283 **Acknowledgments.**

284 We thank two anonymous reviewers for their suggestions. During this research, M. Filippucci was  
285 supported by the Intervention co-financed by the Fund of Development and Cohesion 2007-2013 -  
286 APQ Research - Puglia Region - Regional program to support intelligent specialization and social  
287 and environmental sustainability - FutureInResearch.

288 **References.**

- 289 BAGDASSAROV, N., and H. PINKERTON (2004): Transient phenomena in vesicular lava flows based  
290 on laboratory experiments with analogue materials, *J. Volcanol. Geotherm. Res.*, **132**, 115-136.
- 291 BERNABEU, N., SARAMITO P. AND C. SMUTEK, (2016): Modelling lava flow advance using a  
292 shallow-depth approximation for three-dimensional cooling of viscoplastic flows, *Geological*  
293 *Society, London, Special Publications*, **426** (1):409. <http://dx.doi.org/10.1144/SP426.27>.
- 294 CORDONNIER, B., E. LEV AND F. GAREL, (2015): Benchmarking lava-flow models. From:  
295 Harris, A. J. L., De Groeve, T., Garel, F. & Carn, S. A. (eds) Detecting, Modelling and  
296 Responding to Effusive Eruptions. Geological Society, London, Special Publications, 426,  
297 <http://doi.org/10.1144/SP426.7>
- 298 COSTA, A. AND G. MACEDONIO (2003), Viscous heating in fluids with temperature-dependent  
299 viscosity: implications for magma flows, *Nonlinear Processes in Geophysics*, **10**, 545555.
- 300 COSTA, A. AND G. MACEDONIO (2005a), Viscous heating effects in fluids with temperature  
301 dependent viscosity: triggering of secondary flows, *J. Fluid Mech.*, **540**, 21-38,  
302 DOI:10.1017/S0022112005006075.
- 303 COSTA, A., and G. MACEDONIO (2005b), Computational modeling of lava flows: A review in  
304 Manga, M., and Ventura, G., eds., Kinematics and dynamics of lava flows: *Geological Society*  
305 *of America Special Paper*, **396**, 209218 doi: 10.1130/2005.2396(14)
- 306 COSTA, A., O. MELNIK, AND E. VEDENEVA (2007), Thermal effects during magma ascent in  
307 conduits, *J. Geophys. Res.*, 112B12205, doi:10.1029/2007JB004985
- 308 DIETTERICH, H.R., E., LEV, J., CHEN, J. A. RICHARDSON AND K. V. CASHMAN, (2017):  
309 Benchmarking computational fluid dynamics models of lava flow simulation for hazard  
310 assessment, forecasting, and risk management, *Journal of Applied Volcanology* 6:9 DOI  
311 10.1186/s13617-017-0061-x
- 312 FILIPPUCCI M. (2018), Thermal processes in lava flowing in an open channel, *Nuovo Cimento C-*  
313 *Colloquia and Communications in Physics (in press)*.
- 314 FILIPPUCCI, M., TALLARICO, A., DRAGONI, M. (2017), Viscous dissipation in a flow with power law,  
315 temperature-dependent rheology: Application to channeled lava flows, *J. Geophys. Res.*, **122**  
316 (5), pp. 3364-3378. DOI: 10.1002/2016JB013720
- 317 FILIPPUCCI, M., TALLARICO, A., DRAGONI, M. (2013a), Role of heat advection in a channeled lava  
318 flow with power law, temperature-dependent rheology, *J. Geophys. Res.*, **118** (6), pp. 2764-  
319 2776. DOI: 10.1002/jgrb.50136
- 320 FILIPPUCCI, M., TALLARICO, A., DRAGONI, M. (2013b), Simulation of lava flows with power-law  
321 rheology, *Discrete and Continuous Dynamical Systems - Series S*, **6** (3), pp. 677-685. DOI:  
322 10.3934/dcdss.2013.6.677
- 323 TALLARICO, A., DRAGONI, M., FILIPPUCCI, M., PIOMBO, A., SANTINI, S., VALERIO, A. (2011),  
324 Cooling of a channeled lava flow with non-Newtonian rheology: Crust formation and surface  
325 radiance, *Annals of Geophysics*, 54 (5), pp. 510-520. DOI: 10.4401/ag-5335
- 326 FILIPPUCCI, M., TALLARICO, A., DRAGONI, M. (2011), Conditions for crust and tube formation in lava  
327 flows with power-law rheology, *Bollettino di Geofisica Teorica ed Applicata*, **52** (2), pp. 1-11,  
328 DOI: 10.4430/bgta0008
- 329 FILIPPUCCI, M. (2018), Thermal processes in lava flowing in an open channel, *Il Nuovo Cimento (in*  
330 *press)*.
- 331 FILIPPUCCI, M., TALLARICO, A. AND DRAGONI, M. (2010), A three-dimensional dynamical model for  
332 channeled lava flow with nonlinear rheology, *J. Geoph. Res.*, **115** (5), DOI:  
333 10.1029/2009JB006335

- 334 GRIFFITHS, R. W. (2000). The Dynamics of Lava Flows. *Annual Review of Fluid Mechanics*, **32**(1),  
335 477–518. doi:10.1146/annurev.fluid.32.1.477.
- 336 HOBIGER, M., SONDER, I., BÜTTNER, R. AND ZIMANOWSKI, B. (2011), Viscosity characteristics of  
337 selected volcanic rock melts, *J. Volc. Geoth. Res.*, **200**,1-2 pp.27-34,  
338 doi:10.1016/j.jvolgeores.2010.11.020
- 339 HON, K., J. KAUAHIKAUA, R. DENLINGER AND K. MCKAY (1994): Emplacement and inflation of  
340 pahoehoe sheet flows: observations and measurements of active flows an Kilauea Volcano,  
341 Hawaii, *Geol. Soc. Am. Bull.*, **106**, 351370.
- 342 PATANKAR, S.V. (1980): *Numerical heat transfer and fluid flow*, Series in Computational Methods  
343 in Mechanics and Thermal Sciences, McGraw-Hill.
- 344 PATRICK, M. R. (2004): Numerical modeling of lava flow cooling applied to the 1997 Okmok  
345 eruption: Approach and analysis. *Journal of Geophysical Research*, **109**(B3).  
346 doi:10.1029/2003jb002537
- 347 PINKERTON, H. and R. STEVENSON (1992): Methods of determining the rheological properties of  
348 magmas at sub-solidus temperatures, *J. Volcanol. Geotherm. Res.*, **53**, 47-66.
- 349 SHAW, H.R., T.L. WRIGHT, D.L. PECK and R. OKAMURA (1968): The viscosity of basaltic magma:  
350 An analysis of field measurements in Makaopuhi lava lake, *Hawaii. Am. J. Sci.*, **266**, 255–264.
- 351 SMITH, J.V. (2000): Textural evidence for dilatant (shear thickening) rheology of magma at high  
352 crystal concentrations, *J. Volcanol. Geotherm. Res.*, **99**, 17.
- 353 SONDER I., B. ZIMANOWSKI and R. BÜTTNER (2006): Non-Newtonian viscosity of basaltic magma,  
354 *Geoph. Res. Lett.*, **33**, L02303, doi:10.1029/2005GL024240.
- 355 SPERA J., A. BORGIA, J. STRIMPLE and M. FEIGENSON (1988): Rheology of melts and magmatic  
356 suspensions 1. Design and calibration of concentric cylinder viscosimeter with application to  
357 rhyolitic magma, *J. Geophys. Res.*, **93**, 273-10.
- 358 STEIN, D. J. and F.J. SPERA (1992). Rheology and microstructure of magmatic emulsions: Theory  
359 and experiments, *J. Volcanol. Geotherm. Res.*, **49**, 157–174.
- 360 WHITE, F. M. (2005). *Viscous fluid flow*. New York: McGraw-Hill.

361 **Tables**

<b>Parameter</b>	<b>Description</b>	<b>Value</b>
$a_l$	half channel width	1.5 m
$a$	total width	12 m
$h_l$	channel thickness	1.5 m
$h$	total thickness	6 m
$L$	channel length	100 m
$g$	acceleration of gravity	9.8 m s <sup>-2</sup>
$c_p$	specific heat capacity	837 J kg <sup>-1</sup> K <sup>-1</sup>
$K$	thermal conductivity	3 W K <sup>-1</sup> m <sup>-1</sup>
$T_e$	effusion temperature	1100 °C
$T_s$	solidus temperature	900 °C
$T_w$	wall temperature	30 °C
$k_0$	rheological parameter	1 Pa s <sup>n</sup>
$p_1$	rheological parameter	18.71
$p_2$	rheological parameter	33.4 10 <sup>3</sup> K
$p_3$	rheological parameter	1.35
$p_4$	rheological parameter	0.85 10 <sup>-3</sup> K <sup>-1</sup>
$\alpha$	channel slope	20°
$\epsilon_c$	thermal emissivity	1
$\rho$	density	2800 kg m <sup>-3</sup>
$\sigma$	Stefan constant	5.668108 W m <sup>-2</sup> K <sup>4</sup>
$\chi$	thermal diffusivity	1.28 10 <sup>-6</sup> m <sup>2</sup> s <sup>-1</sup>

362 Table 1. Values of the fixed model parameters

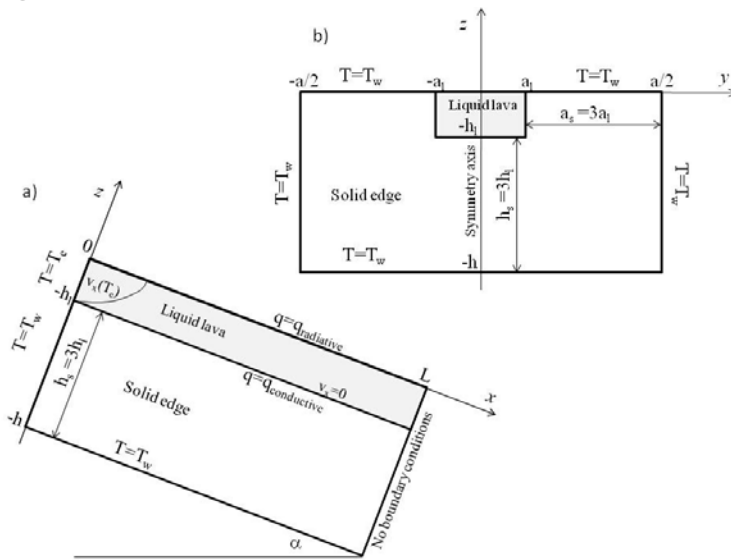


Figure 1. Coordinate system and geometrical parameters. Boundary conditions are also indicated.

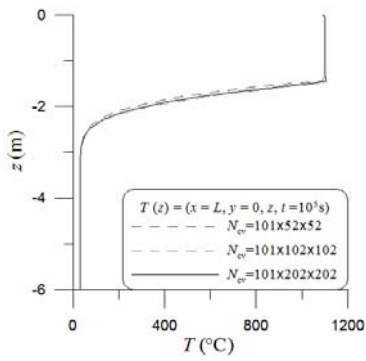


Figure 2. Temperature profile along  $z$  coordinate at  $x=L, y=0, t=10^5$ s, for different mesh sizes, as indicated in the figure legend.

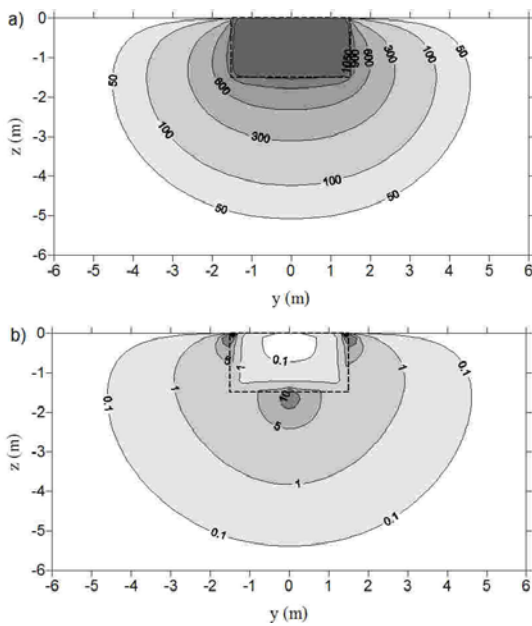
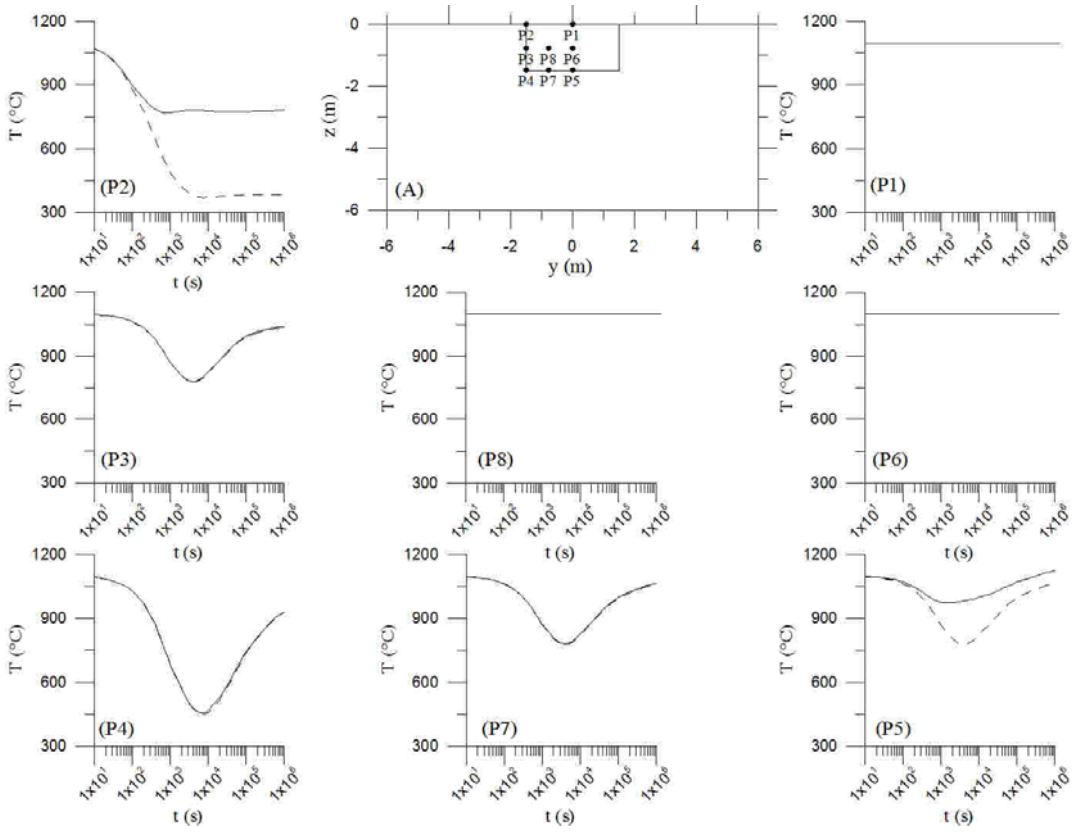


Figure 3. Section map at  $x=L$  and  $t=10^6$ s: a) isolines of temperature  $T$  considering the viscous dissipation term; b) isolines of the temperature difference between the solutions of the heat equation considering the viscous dissipation term and neglecting it. The dashed rectangle indicates the channel section perimeter.



364  
365  
366  
367  
368

Figure 4. Temperature vs time at different monitoring points (P1,...,P8) of the lava channel, as indicated in (A). The label on each plot corresponds to the point in (A). Solid line: solution of the heat equation considering the viscous dissipation term; dashed line: solution of the heat equation neglecting the viscous dissipation term (from Filippucci, 2018).